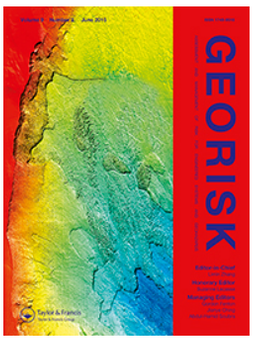

Georisk: Assessment and Management of Risk for Engineered Systems and Geohazards

ISSN: 1749-9518 (Print) 1749-9526 (Online) Journal homepage: http://www.tandfonline.com/loi/ngrk20

A three-level framework for multi-risk assessment

Zhongqiang Liu, Farrokh Nadim, Alexander Garcia-Aristizabal, Arnaud Mignan, Kevin Fleming & Byron Quan Luna

To cite this article: Zhongqiang Liu, Farrokh Nadim, Alexander Garcia-Aristizabal, Arnaud Mignan, Kevin Fleming & Byron Quan Luna (2015) A three-level framework for multi-risk assessment, Georisk: Assessment and Management of Risk for Engineered Systems and Geohazards, 9:2, 59-74, DOI: 10.1080/17499518.2015.1041989

To link to this article: http://dx.doi.org/10.1080/17499518.2015.1041989

Georisk, 2015
Vol. 9, No. 2, 59–74, http://dx.doi.org/10.1080/17499518.2015.1041989

Taylor & Francis
Taylor & Francis Group

A three-level framework for multi-risk assessment

Zhongqiang Liu[a]*, Farrokh Nadim[a], Alexander Garcia-Aristizabal[b], Arnaud Mignan[c], Kevin Fleming[d] and Byron Quan Luna[e]

[a]*Norwegian Geotechnical Institute (NGI), Oslo, Norway;* [b]*Analysis and Monitoring of Environmental Risk (AMRA), Naples, Italy;* [c]*Institute of Geophysics, Swiss Federal Institute of Technology Zurich (ETHZ), Zurich, Switzerland;* [d]*Helmholtz Centre Potsdam, German Research Centre for Geosciences (GFZ), Potsdam, Germany;* [e]*DNV GL, Høvik, Norway*

(*Received 15 February 2015; accepted 14 April 2015*)

The effective management of the risks posed by natural and man-made hazards requires all relevant threats and their interactions to be considered. This paper proposes a three-level framework for multi-risk assessment that accounts for possible hazard and risk interactions. The first level is a flow chart that guides the user in deciding whether a multi-hazard and risk approach is required. The second level is a semi-quantitative approach to explore if a more detailed, quantitative assessment is needed. The third level is a detailed quantitative multi-risk analysis based on Bayesian networks. Examples that demonstrate the application of the method are presented.

Keywords: multi-risk; cascading hazards; time-variant vulnerability; Bayesian network

1. Introduction

Many regions of the world are exposed to and are affected by a number of different types of hazards. The assessment and mitigation of the risk posed by those natural and man-made threats at a given location requires a multi-risk analysis approach that could account for the possible interactions among the threats (multi-hazard), including cascading events and interactions at the vulnerability level (time-variant vulnerability). Performing quantitative multi-risk analysis using the methodologies available today presents many challenges (e.g., Kappes et al. 2012; Marzocchi et al. 2012; Mignan, Wiemer, and Giardini 2014). The risks associated with different types of natural hazards, such as volcanic eruptions, landslides, floods and earthquakes, are often estimated using different procedures, leading to the individual results not being comparable (Marzocchi et al. 2012). Furthermore, the events themselves could be highly correlated (e.g., floods and debris flows could be triggered by an extreme storm event), one type of threat could be the result of another (e.g., a massive landslide that is triggered by an earthquake, a so-called cascade effect) or several independent events may occur at around the same time (e.g., hurricanes and earthquakes). However, it also needs to be kept in mind that the potential losses associated with different hazards when considering their interactions may lead to the situation where their combination is much greater than simply the sum of their parts.

It is obvious that a mathematically rigorous approach to multi-risk assessment that addresses all the challenges named above, as well as the uncertainties in all steps of the analysis, will be complicated and requires considerable resources and expertise (e.g., Komendantova et al. 2014). On the other hand, in many situations, the decision-maker in charge of risk management is constrained to identify the optimum alternatives among those options available, without doing a detailed, rigorous multi-risk analysis. Therefore, the framework recommended in this study is based on a multi-level approach where the decision-maker and/or the risk analyst will not need to use a more sophisticated model than what is required for the problem at hand, or what would be reasonable to use given the available information.

In the following sections, we first outline the concept of multi-hazard assessment and its various components. Next, we deal with time-variant vulnerability. This is followed by a description of the proposed multi-risk analysis framework and the various levels. The multi-risk analysis is then presented, including examples as identified from the EC FP7 Project MATRIX (New Multi-HAzard and MulTi-RIsK Assessment MethodS for Europe). MATRIX (October 2010 to December 2013) set out to develop methodologies and concepts in multi-hazard and risk assessment, considering hazard and vulnerability interactions, as well as the issue of intangible and indirect losses in addition to direct losses.

2. Multi-hazard assessment

The concept of 'multi-hazard assessment' may be understood as the process:

*Corresponding author. Email: zhongqiang.liu@ngi.no

> to determine the probability of occurrence of different hazards either occurring at the same time or shortly following each other, because they are dependent from one another or because they are caused by the same triggering event or hazard, or merely threatening the same elements at risk without chronological coincidence. (European Commission 2010)

From this definition, it is easy to recognise that multi-hazard is a broad concept with different possible interpretations. In general terms, one can split the multi-hazard concept into two possible lines of applications, where multi-hazard assessment may be seen as: (1) the process of assessing different (independent) hazards threatening a given (common) area and (2) a means of identifying and assessing possible interactions and/or cascade effects among the different possible hazardous events.

2.1. Different (independent) hazards threatening a given (common) area

This interpretation of multi-hazard assessment is the most commonly found in the literature. In fact, most of the multi-hazard risk initiatives start from the identification of different hazard sources within a given region of interest and evaluate each individual hazard independently, generally using a hazard-specific assessment methodology. The objective is to identify the spatial distribution of the effects of the different hazards over a range of their respective intensities and to estimate their occurrence probability or return period. The final results, according to the scale of the specific problem, are generally presented as single hazard maps, layers (in a GIS environment), aggregated maps (overlapping all the maps) and hazard curves (for each hazard) that plot the probability (or return period) against the intensity measure of the hazard (e.g., Grünthal et al. 2006; Carpignano et al. 2009; Schmidt et al. 2011).

The main effort within this multi-hazard perspective, as found in the literature, is the harmonisation of the hazard assessment for the different threats. This is generally considered a fundamental requirement in multi-risk analysis to make the risks posed by different threats comparable (e.g., van Westen, Montoya, and Boerboom 2002; Marzocchi et al. 2012, Garcia-Aristizabal et al. 2015). What differentiates the different multi-hazard approaches within this context in the manner in which the harmonisation of the assessment of the different hazards is carried out.

2.2. Hazard interactions, triggering or cascade effects

A multi-hazard assessment considering interaction/triggering effects is, in general, a more demanding process compared with the independent consideration of different hazards. In this type of assessment, the occurrence of one hazardous event could change the probability of occurrence of another event (leading to potential cascades). The typology of interactions that can be grouped under this name are in fact phenomena in which the physical process of interest is a pure triggering mechanism in which an initial event produces a perturbation that, when acting on a given system, may bring it to an unstable state, forcing it to find a new equilibrium state that matches the changing framework conditions (e.g., a new morphological equilibrium after a debris flow event). Reaching this new equilibrium may imply the occurrence of an event that, in this case, may be said to be triggered by the initial one (Gasparini and Garcia-Aristizabal 2014). The link between the intensity of the triggering event (e.g., the ground shaking caused by an earthquake) and the intensity of the triggered event (e.g., a volume of mass moving down a slope) is governed by complex physical mechanisms that are intrinsically related to the specific triggering and triggered events. This fact and the ubiquitous random effects that may affect these processes make probabilistic approaches the most promising way for the quantitative characterisation of such interactions (e.g., Garcia-Aristizabal et al. 2015; Gasparini and Garcia-Aristizabal 2014). In this way, chains of events can be evaluated in probabilistic terms and can be directly integrated into the risk analysis process. For example, Nadim and Liu (2013) and Zhang (2014) approached hazard interactions and performed multi-risk assessment quantitatively using Bayesian networks.

Although most of the multi-risk literature mentions this as an important item to be considered in hazard and risk assessments, the available studies that explicitly consider cascade effects and interactions remain rare (e.g., Marzocchi et al. 2012; Mignan, Wiemer, and Giardini 2014; Gill and Malamud 2014). A possible explanation could be that the necessary input data, and sometimes the complexity of the hazard 'chains' that can be foreseen, often discourage the analyst to consider such interactions and triggering effects in a holistic multi-risk analysis. This view is in agreement with the feedback obtained from civil protection agencies about multi-risk analysis (Komendantova et al. 2014).

3. Time-variant vulnerability

Time-variant (physical and functional) vulnerability considers the evolution of the probable damage to an element at risk over time, including the history of events. Vulnerability, defined as the probability to experience a certain level of damage as a result of a given intensity of a hazard (e.g., peak ground acceleration in the case of earthquakes), evolves due to both physical effects (ageing, corrosion, damage accumulation from past events, etc.) and human actions (reconstruction and

reinforcement, use changes, population settlement evolution, etc.).

Time-variant vulnerability can be considered as the case in which a cluster of hazards (e.g., earthquakes) or the simultaneous occurrence of two or more hazardous events (not necessarily with a direct linkage between them) may imply changes to the vulnerability of the exposed elements, which in the end may also be reflected in the interactions considered in the final risk assessment. Some recent examples in the literature address the increase in a building's vulnerability to ground shaking due to increased structural load following volcanic ash fall or heavy snowfall or after being subjected to a blast (Lee and Rosowsky 2006; Zuccaro et al. 2008; Asprone et al. 2010; Selva 2013). Another well-known situation is the increased vulnerability of structures to successive shaking during an earthquake cluster or sequence (Jalayer et al. 2011; Iervolino, Giorgio, and Chioccarelli 2014). Zhang, Nadim, and Lacasse (2013) proposed a method to estimate the vulnerability factors for loss of life due to three types of sequential or concurrent slide hazards (slides, rockfall and debris flows).

When considering time-variant vulnerabilities in multi-risk analyses, the process of interest is the additive effect of different events acting on the same elements. More specifically, this kind of interaction is referred to in cases where the occurrence of one event (the first one occurring in time) may alter the response of the exposed elements to another event (that may be of the same kind as the former, but may also be of a different type). In general, the physical processes of interest are those related to the response of the system (the exposed element) to the loads caused by different events, taking in account their additive or cumulated effects (Gasparini and Garcia-Aristizabal 2014).

4. Proposed three-level framework for multi-risk assessment

The proposed multi-risk assessment framework is a multi-level process. It assumes that the end user (decision-maker, risk analyst, etc.) has identified the relevant threats and has carried out an assessment of the risk(s) (at the level of sophistication required for the problem at hand) associated with each single hazard(s). Figure 1 shows the general steps of the multi-risk assessment framework presented in this work. The overall multi-risk assessment process comprises the following stages: (1) risk assessment for single hazards, (2) level 1: qualitative multi-risk analysis, (3) level 2: semi-quantitative multi-risk analysis and (4) level 3: quantitative multi-risk analysis. The details are described below.

In the first step, it is assumed that the risk assessment for the single hazard (which may follow a classical approach) is performed taking into account some harmonisation requirements, as those described by the following stages (Figure 2):

- Definition of space/time assessment window (target area, time window) and the risk metric quantifying the expected losses;
- Threat(s) identification (earthquake, flood, volcano, landslide, etc.);
- Single hazard assessment (rate of occurrence, pathway, intensity measure, etc.);
- Assessment of the vulnerability of the elements at risk (people, buildings, etc.);
- Assessment of the consequences in terms of the chosen metric (loss of life, economic losses, environmental degradation, etc.).

Once the results of the single-hazard risk assessment(s) are available, the user embarks upon the three-level process,

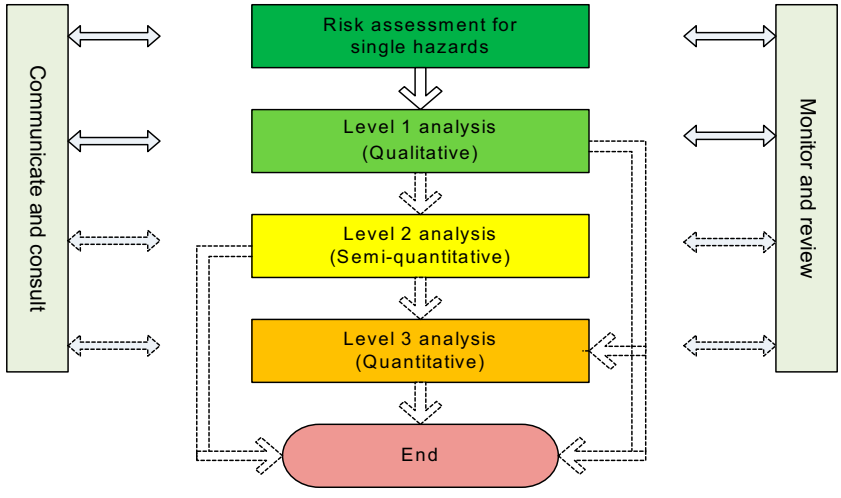

Figure 1. Schematic view of the steps followed in the proposed multi-risk assessment framework.

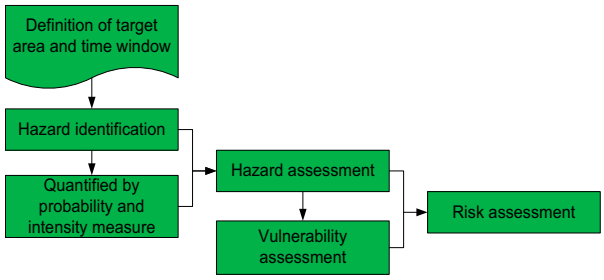

Figure 2. Stages of risk assessment for a single hazard.

which becomes more detailed and rigorous as the user moves from one level to the next. The user moves to a higher level of analysis only if the problem at hand requires a more accurate risk estimate and, equally important, if the data needed for undertaking the more detailed analysis are available. The selection of which of these three levels is to be finally used depends on the outcome of the preliminary risk assessment for the single hazard(s).

4.1. Level 1 analysis

The Level 1 analysis is comprised of a flow chart type list of questions that guides the end user as to whether or not a multi-type assessment approach, which explicitly accounts for cascading hazards and dynamic vulnerability within the context of conjoint or successive hazards, is required. Each question will be supplied with a comprehensive list of answers that the user could choose from. This process is shown schematically in Figure 3.

The flow chart can include, for example, these questions:

- What is the purpose of the risk assessment exercise? (possible answers: identifying the most critical risk scenarios and choosing the optimal risk mitigation measures, assessing the adequacy of resources and level of preparedness for post-event response, etc.)
- Which natural threats are relevant for your area of interest? (possible answers: earthquakes, landslides, volcanic eruptions, tsunamis, wildfires, winter storms, storm surges and coastal floods, fluvial floods, snow avalanches, other perils, etc.)
- If the user has chosen only one natural hazard from the list, how likely is it that the dominant natural threat could happen more than once during the time window of concern with an intensity that will cause significant loss? (possible answers: very likely, likely, unlikely, very unlikely and virtually impossible)

Note that at this stage, if the user has chosen only one natural hazard from the list and chooses very unlikely or virtually impossible as the answer to the above question, then there is no need to go any further and a more detailed multi-risk assessment would be unnecessary:

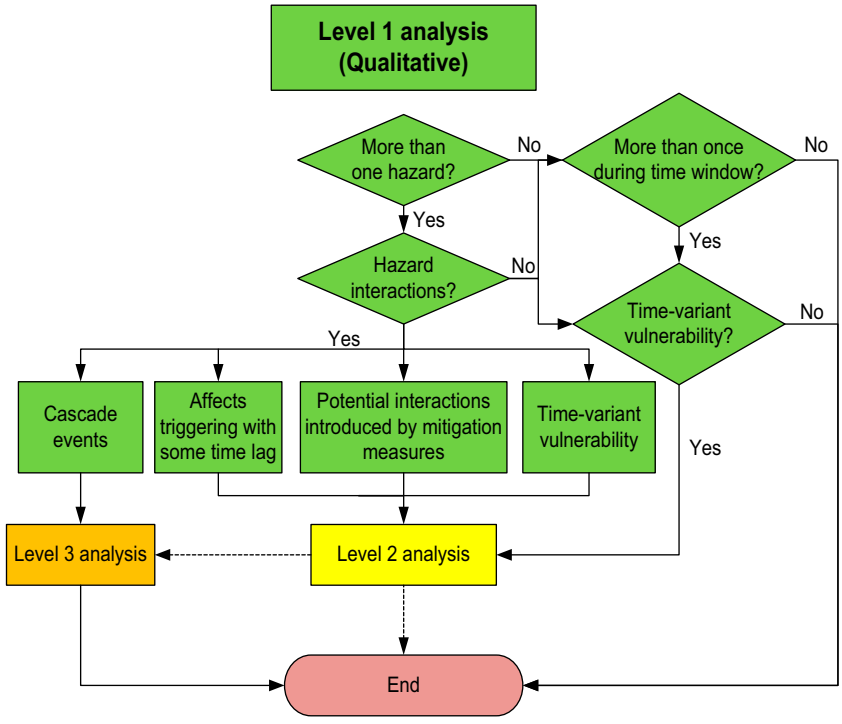

Figure 3. The steps involved in the Level 1 multi-risk analysis.

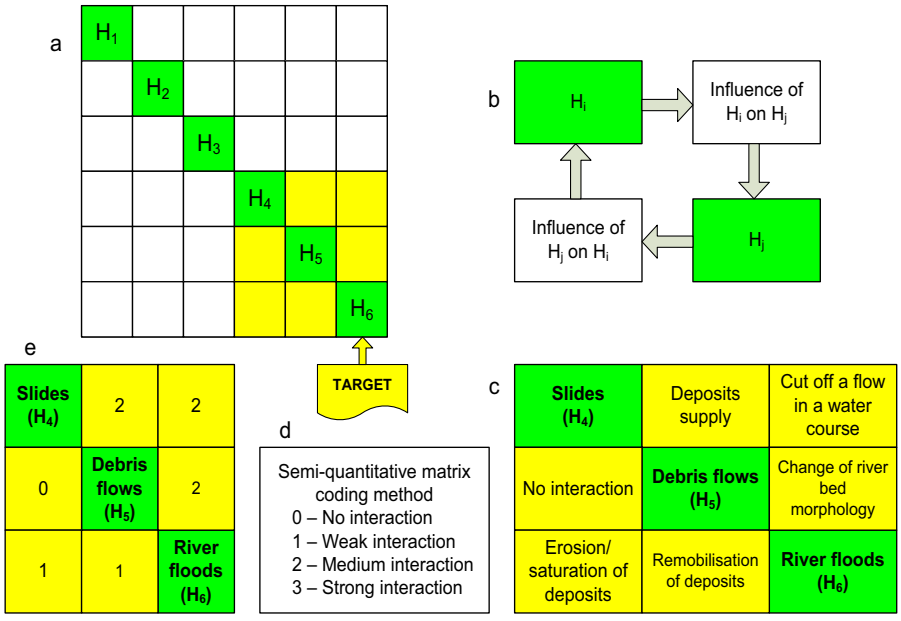

Figure 4. Matrix approach for the identification of the interactions between hazards in the Level 2 analysis (modified after de Simeoni et al. 1999 and Kappes, Keiler, and Glade 2010).

- Cascading events: Could a hazard trigger another hazard in your list (for example: an earthquake triggering a landslide, landslide debris blocking a river and causing flooding when the landslide dam breaks, earthquake causing collapse of flood defence structures and leading to flooding, etc.)? (possible answers: yes or no)
- Conjoint events: Could several hazards in your list occur simultaneously because they are caused by the same external factors (for example: earthquakes and volcanic eruptions are both caused by tectonic processes, winter storms and storm surges, fluvial floods and debris flows caused by extreme precipitation events, etc.), or independently (e.g., hurricanes and earthquakes)? (possible answers: yes or no)
- Dynamic vulnerability: Could the occurrence of one of the hazards in your list significantly influence the vulnerability of some of the elements at risk to another event of the same type or to other hazards (for example: a building partially damaged by an earthquake has a higher vulnerability to the next earthquake or to floods and landslides, ash fall from a volcanic eruption on roof tops will increase the mass and hence may increase its seismic vulnerability, etc.)? (possible answers: yes or no)
- Dynamic hazard: Could the occurrence of one of the hazards in your list significantly influence the occurrence probability of other hazards (for example, a strong earthquake could weaken the soil on a slope and increase the probability of a landslide during extreme precipitation events, etc.)? (possible answers: yes or no)

Additional questions may, of course, be added, depending upon the case of interest. If the results of the Level 1 analysis strongly suggest that a multi-type assessment is required, then the end user moves on to Level 2 to make a first-pass assessment of the effects of dynamic hazard and time-variant vulnerability (see Figure 4). If cascading events are potentially a concern, the user may go directly to the Level 3 analysis.

4.2. Level 2 analysis

In the Level 2 analysis, the interactions among hazards and dynamic vulnerability are assessed approximately using semi-quantitative methods.

To consider hazard interactions and time-variant vulnerability at this level, we suggest a matrix approach based on system theory. This kind of matrix has been used in various fields, including environmental issues (e.g., Simeoni et al. 1999; de Pippo et al. 2008), rock engineering (e.g., Hudson 1992) and natural hazard assessment (Kappes, Keiler, and Glade 2010; Mignan, Wiemer, and Giardini 2014; Gill and Malamud 2014). The basis of this approach consists of the comprehension and description of the relationships among agents and processes in the evolution of the system.

The matrix approach for the identification of the interactions between hazards in the Level 2 analysis is shown in Figure 4. First, a matrix is developed by means of the choice of pairs of hazards, considered as the basic

components of the system (Figure 4a). This is followed by a clockwise scheme of interaction (Figure 4b), with the description of the actual influence between one hazard and another (Figure 4c). More specifically, each element of the row, which crosses one of the hazards in the mean diagonal, shows the influence of this hazard on the system, whereas each element of the column, which crosses the same hazard analysed, shows the influence of the system on this hazard. Considering the descriptions included in each element of the matrix, they are assigned numerical codes varying between 0 (No interaction) and 3 (Strong interaction) with intervals of 1, as a function of their degree of the interaction intensity (Figure 4d and 4e). Once all the hazard-interaction combinations in the matrix are filled, it is possible to verify the degree of the impact of each hazard on the other hazards and the effect on it from other hazards. In order to avoid the excessive weighting of a single hazard, the sum of the codes for the rows and columns is considered. Table 1 shows the coding result for each hazard in the example considered.

In the example presented in Figure 5, it can be seen that landslides have the maximum number of causes and, therefore, they are the dominant hazard caused by other hazards (i.e. the main kind of triggered events). On the other hand, river flooding is in this example the hazard most influencing other hazards, with the maximum number of effects (i.e. the main kind of triggering events).

Using this scoring system, the maximum possible value of each off-diagonal cell in Figure 5a is 3. Therefore, the maximum possible value for the total sum of each row is $3\cdot(n-1)$, where n is the number of hazards. Likewise, the maximum possible value for the total sum of each column is $3\cdot(n-1)$. This means that the maximum possible value for the total sum of causes and effects is:

$$H_{I,\,max} = 2\cdot 3\cdot n\cdot(n-1) = 6\cdot n\cdot(n-1) \qquad (1)$$

where n is the number of hazards and H_I is the hazard interaction index.

Therefore, for the example considered in Table 1, the maximum possible value for the hazard interaction index is $H_{I,\,max}$ = 36. The hazard interaction index can be used as a proxy to assess the potential significance of the interactions; likewise, its value might be used to set a reference threshold supporting the decisional problem of moving to a Level 3 analysis. Given the subjectivity, uncertainties and possible excessive or moderate weighting of single hazards, a subjective threshold hazard interaction index H_{thre} can be defined. In general, a 50% of $H_{I,\,max}$ value can be considered as a conservative threshold for considering a more detailed Level 3 analysis. If the hazard interaction index is less than this threshold, Level 3 analysis is not recommended because the additional accuracy gained by the detailed analyses is most likely within the uncertainty bounds of the simplified multi-risk estimates. Otherwise, Level 3 analysis is recommended. In the example above, the threshold hazard interaction index calculated by Equation (1) is H_{thre} = 18 (50% of 36), while the total value of causes and effects is 16; hence, in the example, we do not need to do Level 3 analysis. The logic of the decisional problem involved in the Level 2 analysis is shown in Figure 5.

Table 1. Coding of each hazard in the system.

Number	Hazard	Causes (Rows)	Effects (Columns)	Causes + effects
1	Landslides	4	1	5
2	Debris flows	2	3	5
3	River floods	2	4	6
Total		8	8	16

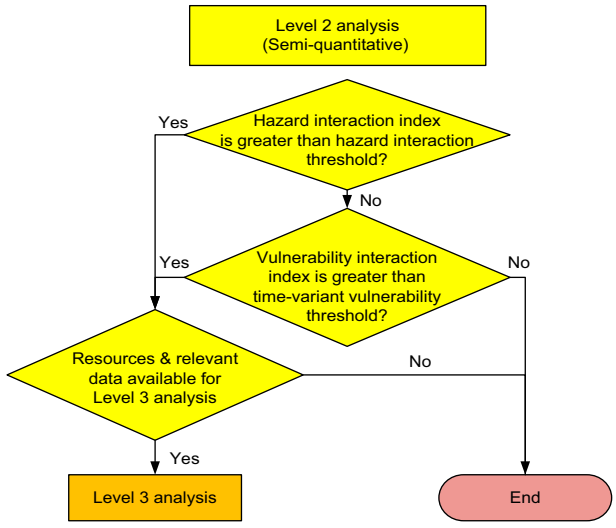

Figure 5. The steps involved in the Level 2 multi-risk analysis.

4.3. Level 3 analysis

In the Level 3 analysis, the effects of interactions among hazards and dynamic vulnerability are assessed quantitatively with high accuracy (as high as the available data allows).

For the Level 3 analysis proposed in this framework, a new quantitative multi-risk assessment model based on Bayesian networks (BaNMuR) is introduced to both estimate the probability of a triggering/cascade effects and model the time-variant vulnerability of a system exposed to multiple hazards. The flexible structure and the unique modelling techniques offered by Bayesian

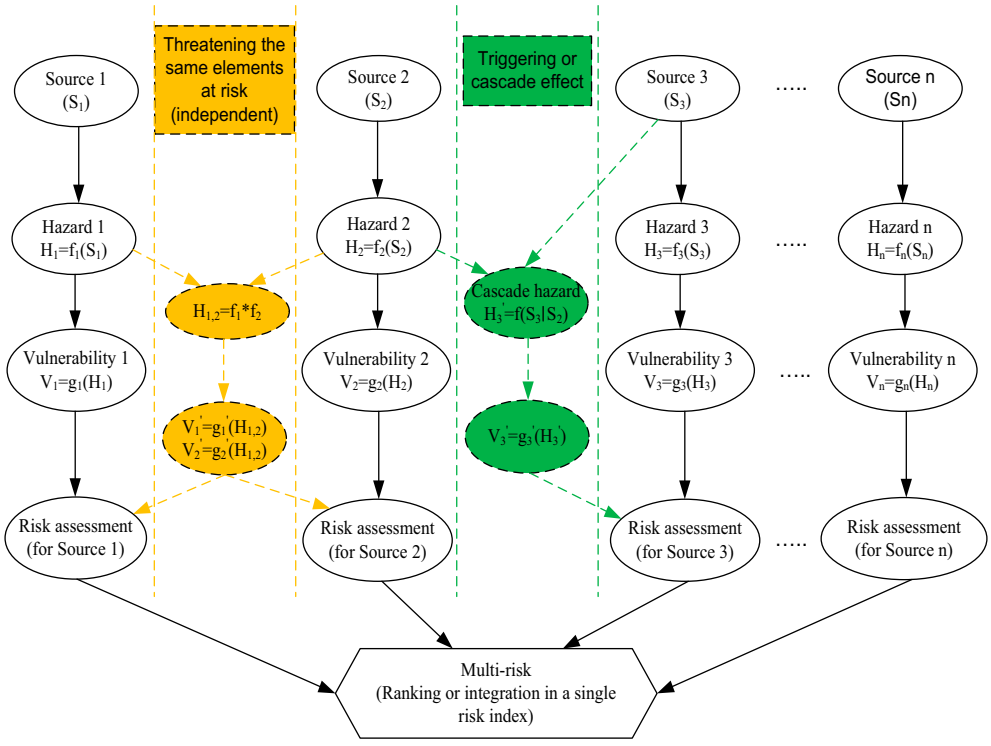

Figure 6. Bayesian network for quantitative multi-risk assessment (modified from Marzocchi et al. 2012).

networks make it possible to analyse interactions and cascading effects, and to handle uncertainties through a simple probabilistic framework. The uncertainties in each hazard/vulnerability and their interrelationships are represented by probabilities. The prior probabilities can be updated with information of specific cases by Bayes' theorem. The uncertainties (mainly epistemic) can be reduced, and the updated multi-risk results could become more reliable based on the new information. In particular, this method is well suited for treating uncertainties associated with hidden geodynamic variables, which are not directly observable (e.g., model uncertainty in causal relationships between unobservable volcanic processes and surface manifestations or monitoring data).

A conceptual Bayesian network multi-risk model may be built as shown in Figure 6. To determine the whole risk from several threats, the network takes into account possible hazards and vulnerability interactions. This would include those events that are:

(1) Independent, but threatening the same elements at risk with or without chronological coincidence (the column marked in deep orange colour in Figure 6);
(2) Dependent on one another or caused by the same triggering event or hazard: this is mainly the case of 'cascading events' (the column marked in green colour in Figure 6).

The network presented consists of two main sub-networks for (1) multi-hazard and (2) time-variant vulnerability, as detailed in the following sections.

4.3.1. Multi-hazard analyses

A number of possible scenarios for single hazards and cascade events have been identified for the case study examples identified in the MATRIX project (Garcia-Aristizabal et al. 2012). A Bayesian network as that shown in Figure 7 may be built to describe the interactions between hazards. It is obvious that one hazardous event could trigger a number of other hazardous events.

Once the propagation pattern of the cascade effect is known, the occurrence probability of the cascade effect can be estimated. Generally, the probability of the cascade effect ($P_{cascade}$) is calculated as the multiplication of the probability of the primary event ($P_{primary}$) and the conditional probability of the impacted events ($P_{conditional}$):

$$P_{cascade} = P_{primary} \times P_{conditional} \quad (2)$$

4.3.2. Time-variant vulnerability assessment

Predicting the damage to the elements at risk (e.g., buildings) is critical for the evaluation of economic losses and should be estimated with an acceptable degree of credibility in order to determine the potential losses that are dependent upon the performance of those

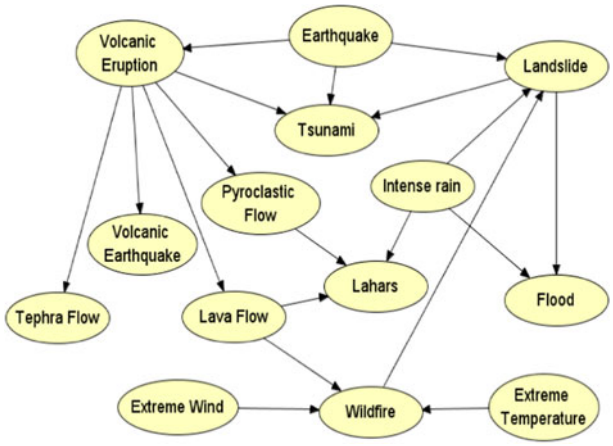

Figure 7. Possible scenarios of multi-hazard interaction, as considered during the MATRIX project (redrawn from Garcia-Aristizabal et al. 2012).

elements subjected to various hazard excitations. Fragility curves represent the cumulative distribution of damage, which specify the continuous probability that the indicated damage-state has been reached or exceeded, and could provide graphical information on the distribution of damage.

The limit state (LS) probability for a structure exposed to a single hazard can be expressed in terms of discrete random variables as follows (Lee and Rosowsky 2006):

$$P_f = \sum_{i=0}^{\infty} P[LS|I=i]P[I=i] = \sum_{x=0}^{\infty} P[D>C|I=i]P[I=i] \quad (3)$$

where I is the intensity measure of the hazard and LS (limit state) is the condition in which the load demand due to the hazard is greater than the capacity C. The conditional probability P[$LS \mid I = i$] is the probability of reaching LS at a given hazard intensity level, $I = i$. The term P[$I = i$] is the marginal hazard probability. For continuous random variables, Equation (3) can be expressed as:

$$P_f = \int_{i=0}^{i=\infty} F_r(i) g_I(i) di \quad (4)$$

where $F_r(i)$ is the fragility function in the form of a cumulative distribution function and $g_I(i)$is the hazard function in the form of a probability density function.

In the case of a structure subjected to a multi-hazard situation involving additive load effects (e.g., earthquake + landslide), the convolution concept must be expanded. This multi-hazard form is calculated as:

$$\begin{aligned} P_f &= \sum_{i_1=0}^{\infty}\sum_{i_2=0}^{\infty}\ldots\sum_{i_n=0}^{\infty} P[LS|I_1 = i_1 \bigcap I_2 \\ &= i_2 \bigcap \ldots \bigcap I_n = i_n] \times P[I_1 = i_1 \bigcap I_2 \\ &= i_2 \bigcap \ldots \bigcap I_n = i_n] \end{aligned} \quad (5)$$

Equation (4) can also be expressed in terms of continuous random variables, which for the case of independent hazards read as:

$$P_f = \int_{i_1=0}^{i_1=\infty}\int_{i_2=0}^{i_2=\infty}\ldots\int_{i_n=0}^{i_n=\infty} F_r(LS|i_1,i_2\ldots,i_n) g_{I_1}(i_1) g_{I_2}(i_2) \ldots g_{I_n}(i_n) di_1 di_2 \ldots di_n \quad (6)$$

It is worth noting that in the case of dependent hazards, the hazard terms $g_{In}(i_n)$ in Equation (6) should be properly considered. For example, in the case of two dependent events, it is necessary to consider that $p(I_2 \bigcap I_1) = p(I_2|I_1)p(I_1)$ (see, e.g., Gasparini and Garcia-Aristizabal 2014).

Figure 8 shows an example of seismic fragility curves for a low rise, low code RC building at the yield (green) and collapse (red) LSs versus the peak ground acceleration (PGA) (Tsionis, Papailia, and Fardis 2011).

For the debris flow fragility curve (Figure 9), we adopt the example provided by Fuchs, Heiss, and Hubl (2007), expressed as:

$$V = 0.11h^2 - 0.22h \quad (7)$$

where V is the debris flow vulnerability and h is deposition height, in metre.

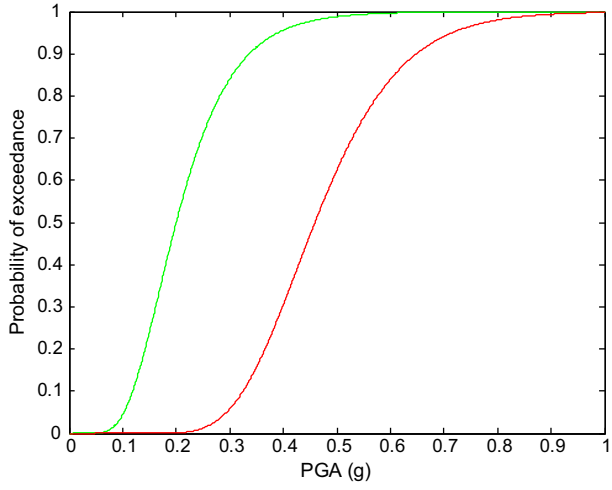

Figure 8. Seismic fragility curves for a low rise, low code RC building for the yield (green curve) and collapse (red curve).

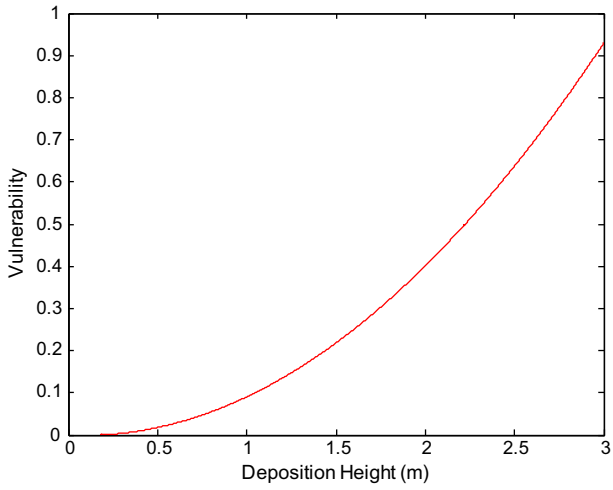

Figure 9. Debris flow fragility curve.
Source: Fuchs, Heiss, and Hubl 2007.

In the case of a system subjected to two hazards (as is the case with earthquakes and debris flow load considered in this study), an alternative formulation must be sought such that the fragility is expressed in terms of the two demands (hazards). When the vulnerabilities to the hazards are completely independent, the multi-hazard vulnerability factor will be one minus the probability that the building has not collapsed after having been exposed to the two hazards one after the other:

$$1 - P_f = \left(1 - P_{f1}\right)\left(1 - P_{f2}\right) \tag{8}$$

where P_f is the LS probability for the building exposed to two hazards, and P_{f1} and P_{f2} are the LS probabilities for the building at given hazard intensity measures due to hazards H_1 and H_2, respectively.

Figure 10 shows an example of seismic fragility surface calculated considering debris flow loads. As can be seen, these fragilities are presented over three dimensions, where the x-axis is the peak ground acceleration, the y-axis is the deposition height and the z-axis is the probability of reaching a given LS.

4.3.3. Multi-risk assessment

The expected risk of the exposed elements (e.g., buildings) subjected to potential hazards, assuming that the intensity measure as the hazard parameter is deterministic, can be calculated as:

$$R = P \times L \tag{9}$$

where P is the probability of the occurrence of damage and L indicates the corresponding loss. The equation shows that any factor which alters either the probability or the value of the resulting loss affects the related risk. Diverse damage states and associated loss values, Li (i = 1 to the number of probable damage states), with a different probability of occurrence, and Pi, may be envisaged for the elements at risk. The probable risk of the system, R, can then be estimated as the summation of

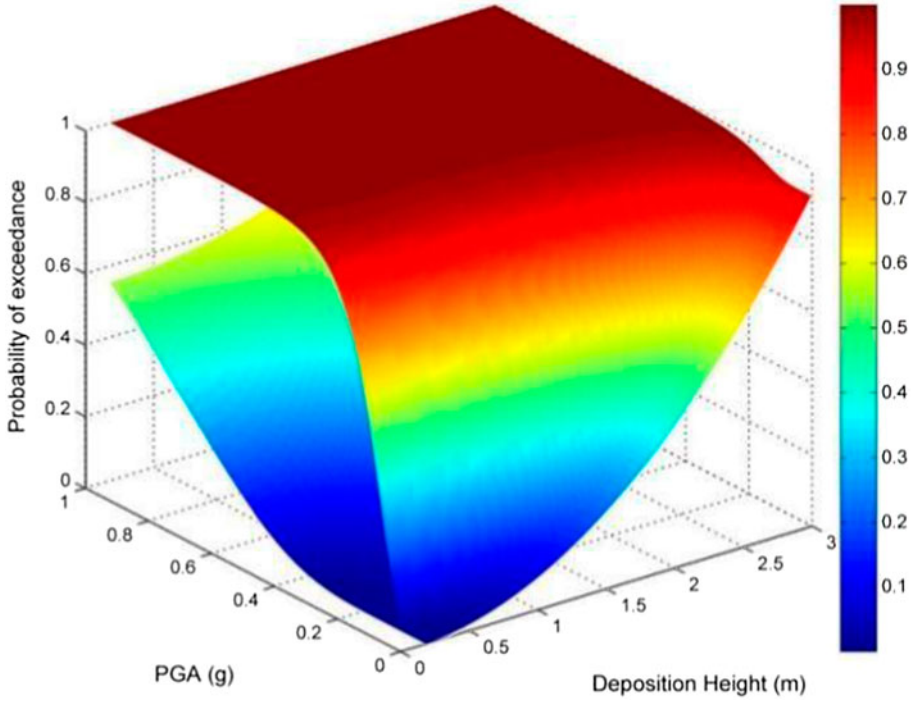

Figure 10. Fragility surface for a scenario involving a seismic event and debris flow for a low rise, low code RC building.

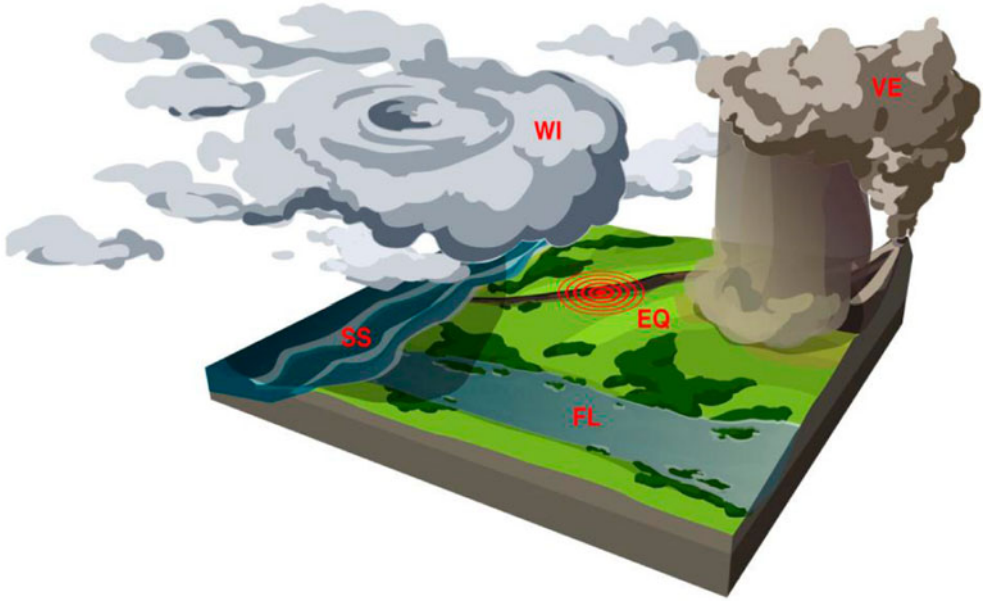

Figure 11. Principal sketch of the Virtual City region as developed within the MATRIX project, redrawn from Mignan (2013). Note: EQ, Earthquake; FL, Flood; SS, Sea submersion; VE, Volcanic eruption; and WI, Wind.

the loss of each damage state:

$$R = \sum P_i \times L_i \tag{10}$$

5. Example of quantitative multi-risk assessment

The case described here is based on the Virtual City database, as shown in Figure 11, developed within the scope of the MATRIX project (Mignan 2013; Komendantova et al. 2014).

The Virtual City (Mignan 2013) considers a 100 km by 100 km region threatened by various natural hazard types. The elements at risk consist of 50,000 identical low rise concrete buildings distributed within a 20 km by 20 km area inside the Virtual Region (Figure 12). The average rebuilding cost per unit for the 'collapse' damage state of these buildings is assumed to be 200,000 Euro, and the average repair costs for the 'yielding' damage state as 50% of the unit rebuilding cost. The earthquake source zone is a 45-km-long linear source (black line in Figure 12), where the start and end points are (0.3, 38.8) and (35, 65), respectively.

This case is used to explain how to perform multi-risk assessment within a complicated system based on the BaNMuR model described above. Therefore, it is not a validation of the performance of the model. The case partly makes use of artificial data (including the earthquake source) and partly typical engineering values (as for the soil parameters and rainfall intensity). The scenarios consider debris flows triggered by both earthquake and precipitation. We take one cell for example, the central coordinate of which is (40.005, 40.005).

5.1. Constructing causal networks for multi-risk assessment

A Bayesian network is built with the program Bayes Net Toolbox (Murphy 2001) on the basis of the MATrix LABoratory (MATLAB) suite, as shown in Figure 13. There are 17 nodes and 19 arcs in the network. The network consists of five main sub-networks for seismic hazard, cascade effect, debris flow hazard, building damage and risk assessment.

5.2. Quantifying the networks

5.2.1. Seismic hazard sub-network

To predict peak ground acceleration at a given site, the distribution of distances from the earthquake epicentre to the site of interest is necessary. The seismic sources are defined by epicentres that are assumed to have equal probability. In the Virtual City, these equal probability locations fall along the line that defines the fault. Using the geometric characteristics of the source, the distribution of the distances can be calculated as shown in Figure 14.

The distribution of earthquake magnitudes in a given region follows a distribution observed by Gutenberg and Richter (1944):

$$\log \lambda_m = a - bM \tag{11}$$

where λ_m is the rate of earthquakes with magnitudes greater than M, and a and b are constants that are generally estimated using statistical analyses of historical observations.

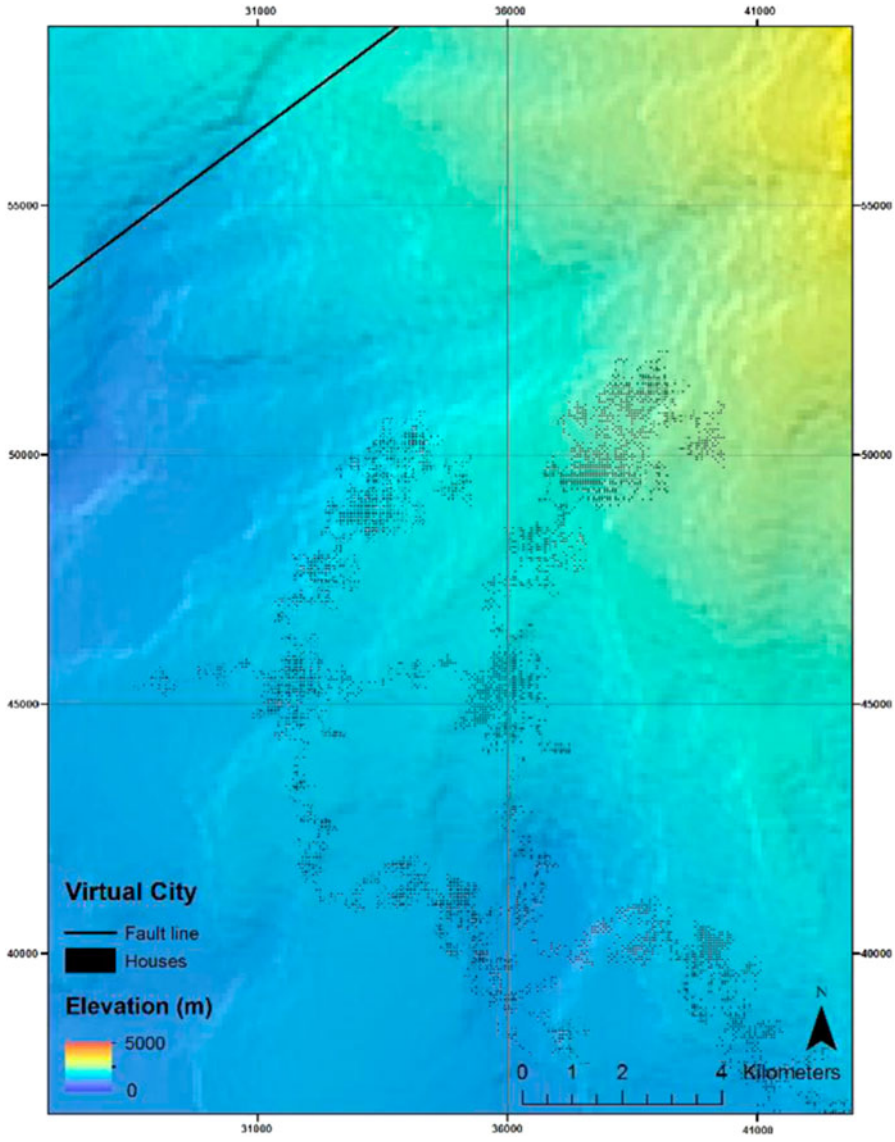

Figure 12. Example locations of the 50,000 buildings and the earthquake source in the MATRIX Virtual City region.

The above-described Gutenberg–Richter recurrence law is generally applied with a lower and upper bound. The lower bound is represented by a minimum magnitude m_{min} below which earthquakes are ignored due to their lack of engineering importance (usually $m_{min} = 4$). The upper bound is given by the maximum magnitude m_{max} that a given seismic source can produce, following the empirical relationship of Wells and Coppersmith (1994):

$$m_{\max} = 5.08 + 1.16\log_{10}(L) \tag{12}$$

where L is the length of the line source. On the basis of the equation above, the line source can produce a maximum magnitude of 7.0.

Setting a range of magnitudes of interest, using the bounds m_L and m_U, Equation (13) can be used to compute the probability that an earthquake magnitude falls within these bounds (Figure 15):

$$P(m_L \le M \le m_U | m_{\min} \le M \le m_{\max}) = \frac{\lambda_{m_L} - \lambda_{m_U}}{\lambda_{m_{\min}} - \lambda_{m_{\max}}} \tag{13}$$

The conditional probabilities of PGA given the magnitude and distance to the epicentre are calculated based on the ground motion prediction equation proposed by Ambraseys et al. (2005) and using a Monte Carlo simulation. The resulting seismic hazard curve is shown in Figure 16.

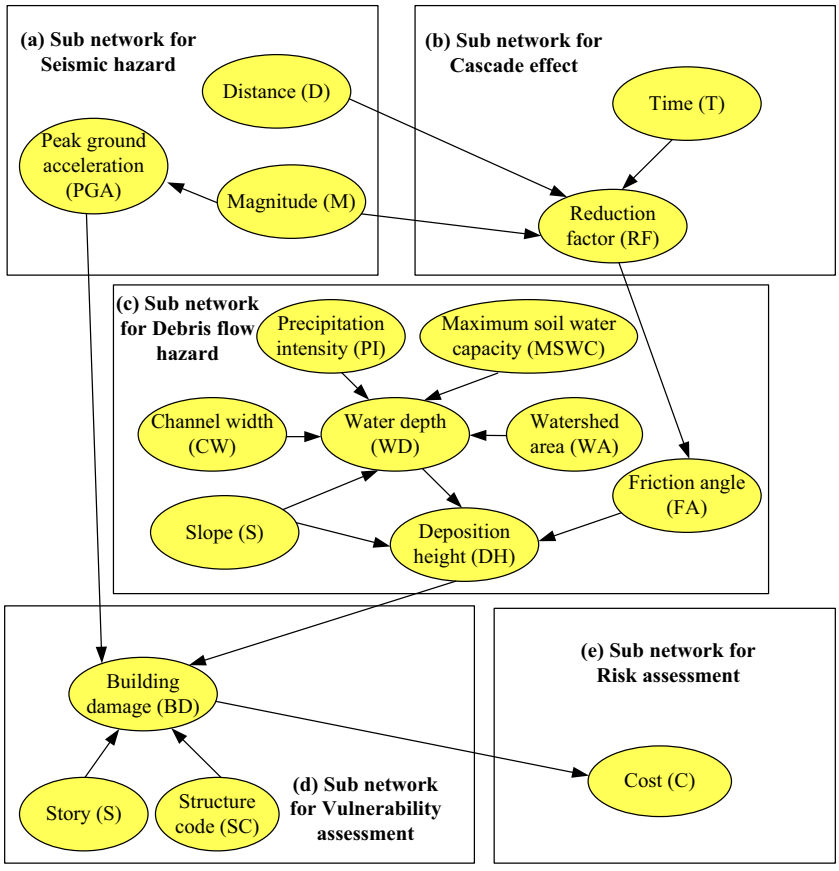

Figure 13. The Bayesian network for a multi-risk assessment considering earthquakes and debris flow.

5.2.2. *Cascade effect sub-network*

Soil properties can be influenced by earthquakes. Post-earthquake soil strengths may be lower than the pre-earthquake (static) strengths for zones that are susceptible to strength loss. As time passes, the progression of soil self-healing will result in increased shear strength compared to that shortly after the earthquake. According to Luna et al. (2013), the reduction factor (*RF*) of soil shear strength f_s can be calculated as:

$$f_s = \frac{(\tan\phi')_{After}}{(\tan\phi')_{Before}} = \frac{\gamma_s d_b - \gamma_w d_b}{\gamma_s d_b - \gamma_w d_b + \gamma_w d_w \cdot \frac{1}{1+e^{-1.3M+9.5}} \cdot 10^{-70000M^{-8.1}D} \cdot e^{-0.5T}} \tag{14}$$

where ϕ' is the effective internal friction angle of the soil, d_b is the depth of the failure surface, d_w is the water table depth, γ_s is the soil unit weight, γ_w is the specific weight of water, D is the distance to the epicentre, T is the time after the earthquake and M is the earthquake magnitude. The values of these properties for sandy soil following an earthquake are listed in Table 2.

Using the values listed in Table 2, Equation (14) can be simplified to become,

$$f_s = \frac{2}{2 + 0.6 \cdot \frac{1}{1+e^{-1.3M+9.5}} \cdot 10^{-70000M^{-8.1}D}} \tag{15}$$

The conditional probabilities of the *RF* given the magnitude and distance to epicentre are calculated using again a Monte Carlo simulation, the results shown in Figure 17.

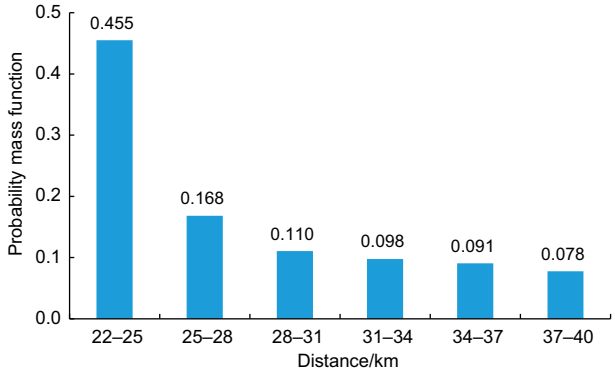

Figure 14. Specification of the discrete probabilities of distance.

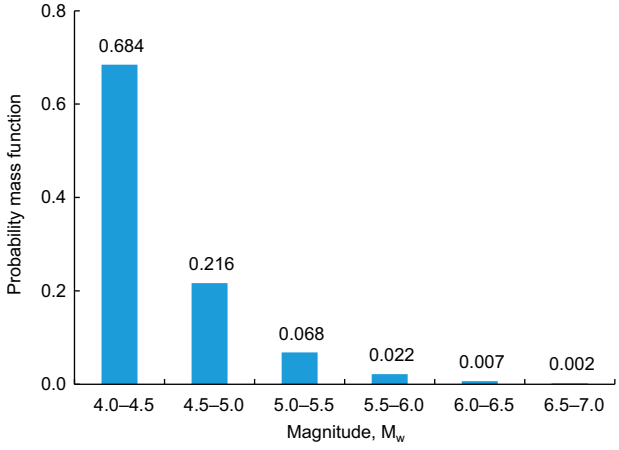

Figure 15. Specification of the discrete probabilities of magnitude.

5.2.3. Debris flow hazard sub-network

Takahashi (1991) proposed a comprehensive theory behind the mechanism of debris flow dynamics. The debris flow deposition height DH can be quantified as:

$$DH(WD, FA, S) = WD\left[k_1\left(\frac{\tan FA}{\tan S} - 1\right) - 1\right]^{-1} \quad (16)$$

where $k_1 = C_b(d_b - 1)$ with $d_b \approx 2.65$, the relative density of the grains, and $C_b \approx 0.7$, the volumetric concentration of the sediments. The other variables represent the factors outlined in Figure 13.

The watershed area, channel width, slope angle and maximum soil water capacity used herein are shown in Table 3, while the precipitation intensity properties are listed in Table 4.

The debris flow hazard curve can therefore be calculated, as shown in Figure 18.

5.2.4. Building damage sub-network

As introduced in Section 4.3.2, the fragility surface for the RC building subject to earthquake and debris flow can be obtained. The classes of building examined in terms of their storeys include low rise, medium rise and high rise, while the states of structure code are low, medium and high. In the following, only results for a low rise, low code building located in the grid specified above are considered.

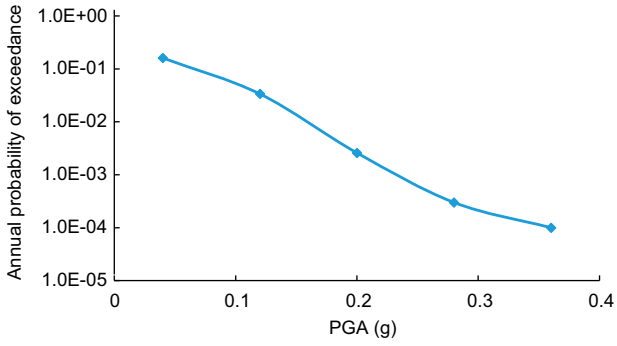

Figure 16. Specification of the discrete probabilities of PGA.

Table 2. Sandy soil properties at a given time following an earthquake.

Water unit weight γ_w (N/m^3)	9800	Ground water depth d_w (m)	1
Soil unit weight γ_s (N/m^3)	20,000	T(year)	1
Failure depth d_b(m)	2	Tangent of effective internal friction angle tan ϕ'	0.9

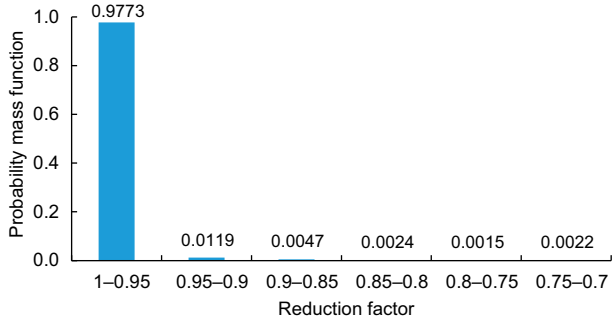

Figure 17. Specification of the discrete probabilities of the RF for sandy soil after an earthquake using the values listed in Table 2.

Table 3. Detailed information of the debris flow's initiation area.

Watershed area WA (m^2)	2,000,000	Maximum soil water capacity$MSWC$ (m/s)	5×10^{-9}
Channel width CW (m)	2	Tangent of slope angle tan S	0.2

Table 4. Precipitation intensity properties.

Return period (years)	Annual frequency	Precipitation intensity (m/s)
1.35	0.7389	0.000002
5	0.2	0.000005
20	0.05	0.00001
100	0.01	0.000015
1000	0.001	0.00002
10,000	0.0001	0.000025

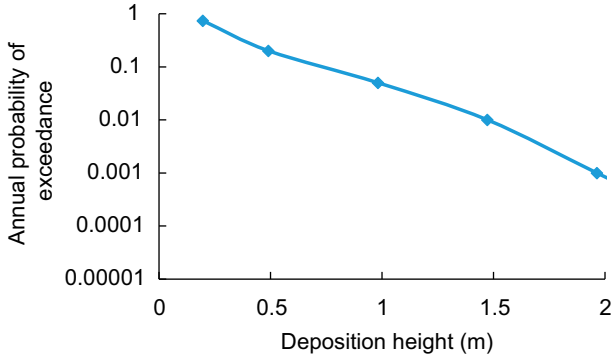

Figure 18. Specification of the exceedance probabilities of deposition height.

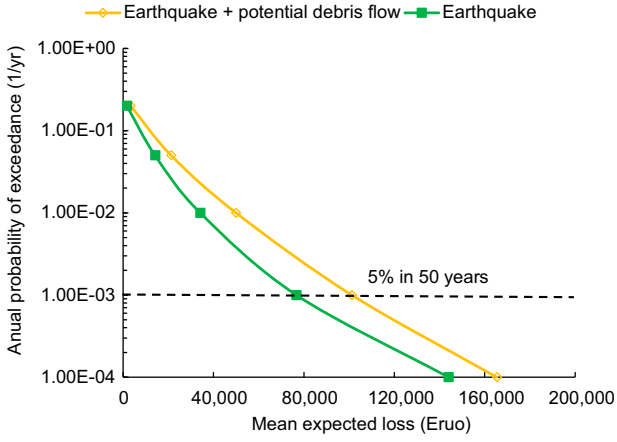

Figure 19. Risk curves for the selected site.

5.3. Results

Figure 19 shows the loss hazard curves giving the annual frequency of exceeding various levels of economic loss in terms of a low rise, low code building when exposed to earthquake hazard and multi-hazard (earthquake and potential debris flow hazard) scenarios at selected site. It is worth noting that the mean expected loss will increase with respect to the same return period, when taking into account cascade effects (i.e., sub-network for cascade effect in Figure 13b). For instance, the 5% probability of exceedance in 50-year curves shown has loss values of approximately 77,000 Euro and 100,000 Euro when considering earthquake hazard and both earthquake and potential debris flow hazards, respectively.

6. Conclusions

Quantification of all the natural and anthropogenic risks that can affect an area of interest is a basic factor for the development of a sustainable environment, land-use planning and risk mitigation strategies. In this study, we put forward a consistent framework for multi-risk assessment. The developed procedure consists of three levels: (1) Level 1: qualitative analysis, (2) Level 2: semi-quantitative analysis and (3) Level 3: quantitative analysis.

The qualitative analysis at Level 1 comprises a flow chart algorithm and allows the end user to decide whether or not a more quantitative multi-risk assessment is required. In the semi-quantitative Level 2 analysis, the interactions among hazards and dynamic vulnerability are assessed using qualitative and semi-quantitative methods. To consider hazard interactions and time-variant vulnerability at this level, a matrix approach method based on system theory is suggested. In the quantitative Level 3 analysis, the effects of interactions among hazards and dynamic vulnerability are assessed quantitatively with a high accuracy. In this case, a quantitative multi-risk assessment model based on Bayesian networks is introduced to both estimate the probability of a triggering/cascade effects and model the time-variant vulnerability of a system exposed to multiple hazards. The flexible structure and the unique modelling techniques offered by Bayesian networks make it possible to analyse interactions and cascading effects using a simple probabilistic framework. In this way, multi-risk assessment can be performed step by step. At the same time, the interactions among different threats are considered in a systematic way in a harmonised structure in the recommended framework.

Disclosure statement

No potential conflict of interest was reported by the authors.

References

Ambraseys, N. N., J. Douglas, S. K. Sarma, and P. M. Smit. 2005. "Equations for the Estimation of Strong Ground Motions from Crustal Earthquakes Using Data from Europe and the Middle East: Horizontal Peak Ground Acceleration and Spectral Acceleration." *Bulletin of earthquake engineering* 3 (1): 1–53. doi:10.1007/s10518-005-0183-0.

Asprone, D., F. Jalayer, A. Prota, and G. Manfredi. 2010. "Proposal of a Probabilistic Model for Multi-hazard Risk Assessment of Structures in Seismic Zones Subjected to Blast for the Limit State of Collapse." *Structural Safety* 32 (1): 25–34. doi:10.1016/j.strusafe.2009.04.002.

Carpignano, A., E. Golia, C. Di Mauro, S. Bouchon, and J.-P. Nordvik. 2009. "A Methodological Approach for the Definition of Multi-risk Maps at Regional Level: First Application." *Journal of Risk Research* 12 (3–4): 513–534. doi:10.1080/13669870903050269.

De Pippo, T., C. Donadio, M. Pennetta, C. Petrosino, F. Terlizzi, and A. Valente. 2008. "Coastal Hazard Assessment and Mapping in Northern Campania, Italy." *Geomorphology* 97 (3–4): 451–466. doi:10.1016/j.geomorph.2007.08.015.

European Commission. 2010. "Commission Staff Working Paper: Risk Assessment and Mapping Guidelines for Disaster Management." Brussels: European Commission.

Fuch, S., K. Heiss, and J. Hubl. 2007. "Towards an Empirical Vulnerability Function for Use in Debris Flow Risk Assessment." *Natural Hazards and Earth System Science* 7 (5): 495–506. doi:10.5194/nhess-7-495-2007

Garcia-Aristizabal, A., P. Gasparini, and G. Uhinga. 2015. "Multi-risk Assessment as a Tool for Decision-making." In *Climate Change and Urban Vulnerability in Africa, A Multidisciplinary Approach*. edited by S. Pauleit, G. Jorgensen, Kabisch, P. Gasparini, S. Fohlmeister, I. Simonis, K. Yeshitela, A. Coly, S. Lindley, W. J. Kombe, 229–258. Future Cities, Vol. 4, Springer International Publishing. doi:10.1007/978-3-319-03982-4_7

Garcia-Aristizabal, A., W. Marzocchi G. Woo, A. Reveillere, J. Douglas, G. Le Cozannet, F. Rego, C. Colaco, K. Fleming, M. Pittore, S. Tyagunov, S. Vorogushyn, F. Nadim, B. V. Vangelsten, and W. ter Horst). 2012. "Review of existing procedures for multi-hazard assessment, Deliverable D3.1." *New methodologies for multi-hazard and multi-risk assessment methods for Europe (MATRIX)*, contract No. 265138.

Gasparini, P., and A. Garcia-Aristizabal. 2014. "Seismic Risk Assessment, Cascading Effects." In *Encyclopedia of Earthquake Engineering, SpringerReference*, edited by M. Beer, E. Patelli, I. Kougioumtzoglou, I. Au, 1–20. Springer Berlin Heidelberg. doi:10.1007/978-3-642-36197-5_260-1

Gill, J. C., and B. D. Malamud. 2014. "Reviewing and Visualizing the Interactions of Natural Hazards." *Reviews of Geophysics* 52 (4): 680–722. doi:10.1002/2013RG000445.

Grünthal, G., A. H. Thieken, J. Schwarz, K. S. Radtke, A. Smolka, and B. Merz. 2006. "Comparative Risk Assessments for the City of Cologne – Storms, Floods, Earthquakes." *Natural Hazards* 38: 21–44, doi:10.1007/s11069-005-8598-0.

Gutenberg B., and C. F. Richter. 1944. "Frequency of Earthquakes in California." *Bulletin of the Seismological Society of America* 34: 185–188.

Hudson, J. A. 1992. *Rock Engineering System*. Chichester: Ellis Horwood..

Iervolino, I., M. Giorgio, and E. Chioccarelli. 2014. "Closed-form Aftershock Reliability of Damage-cumulating Elastic-perfectly-plastic Systems." *Earthquake Engineering Structural Dynamics* 43 (4): 613–625. doi:10.1002/eqe.2363.

Jalayer F., D. Asprone, A. Prota, and G. Manfredi. 2011. "A Decision Support System for Post-earthquake Reliability Assessment of Structures Subjected to Aftershocks: An Application to L'Aquila Earthquake, 2009." *Bulletin of Earthquake Engineering* 9 (4): 997–1014. doi:10.1007/s10518-010-9230-6.

Kappes, M. S., M. Keiler, and T. Glade. 2010. "From Single- to Multi-hazard Risk Analyses: A Concept Addressing Emerging Challenges. In *Mountain Risks: Bringing Science to Society. Proceedings of the International Conference*, edited by J.-P. Malet, T. Glade, and N. Casagli, 351–356. Florence: CERG Editions.

Kappes, M. S., M. Keiler, K. von Elverfeld, and T. Glade. 2012. "Challenges of Analyzing Multi-hazard Risk: A Review." *Natural Hazards* 64 (2): 1925–1958. doi:10.1007/s11069-012-0294-2.

Komendantova, N., R. Mrzyglocki, A. Mignan, B. Khazai, F. Wenzel, A. Patt, and K. Fleming. 2014. "Multi-hazard and Multi-risk Decision-support Tools as a Part of Participatory Risk Governance: Feedback from Civil Protection Stakeholders." *International Journal of Disaster Risk Reduction* 8: 50–67. doi:10.1016/j.ijdrr.2013.12.006.

Lee, K. H., and D. V. Rosowsky. 2006. "Fragility Analysis of Woodframe Buildings Considering Combined Snow and Earthquake Loading." *Structural Safety* 28 (3): 289–303. doi:10.1016/j.strusafe.2005.08.002

Luna B. Q., B. V. Vangelsten, Z. Q. Liu, U. Eidsvig, and F. Nadim. 2013. "Landslides Induced by the Interaction of an Earthquake and Subsequent Rainfall-A Spatial and Temporal Model." *Proccedings of 18th International Conference on Soil Mechanics and Geotechnical Engineering*, Paris, September 2–6.

Marzocchi, W., A. Garcia-Aristizabal, P. Gasparini, M. L. Mastellone, and A. Di Ruocco. 2012. "Basic Principles of Multi-risk Assessment: A Case Study in Italy." *Natural Hazards* 62 (2): 551–573. doi:10.1007/s11069-012-0092-x.

Mignan A. 2013. D7.2 MATRIX-CITY User Manual, New Methodologies for Multi-hazard and Multi-risk Assessment Methods for Europe, Deliverable 7.2. 78. accessed December, 2014. http://matrix.gpi.kit.edu/downloads/MATRIX-D7.2.pdf.

Mignan, A., S. Wiemer, and D. Giardini. 2014. "The Quantification of Low-probability–high-consequences Events: Part I. A Generic Multi-risk Approach." *Natural Hazards* 73 (3): 1999–2022. doi:10.1007/s11069-014-1178-4.

Murphy, K. 2001. "The Bayes Net Toolbox for Matlab." *Computing Science and Statistics* 33: 331–350.

Nadim, F., and Z. Q. Liu. 2013. "Quantitative risk assessment for earthquake-triggered landslides using Bayesian network." *Proccedings of 18th International Conference on Soil Mechanics and Geotechnical Engineering*, Paris, September 2–6.

Schmidt, J., I. Matcham, S. Reese, A. King, R. Bell, R. Henderson, G. Smart, J. Cousins, W. Smith, and D. Heron. 2011. "Quantitative Multi-risk Analysis for Natural Hazards: A Framework for Multi-risk Modelling." *Natural Hazards* 58 (3): 1169–1192. doi:10.1007/s11069-011-9721-z.

Simeoni, U., G. Calderoni, U. Tessari, and E. Mazzini. 1999. "A New Application of System Theory to Foredunes Intervention Strategies." *Journal of Coastal Research* 15 (2): 457–470.

Selva, J. 2013. "Long-term Multi-risk Assessment: Statistical Treatment of Interaction among Risks." *Natural Hazards* 67 (2): 701–722. doi:10.1007/s11069-013-0599-9.

Takahashi, T. 1991. *Debris Flow*. Rotterdam: A. A. Balkama. IAHR Monograph.

Tsionis G., A. Papailia, and M. N. Fardis. 2011. "Analytical Fragility Functions for Reinforced Concrete Buildings and Buildings Aggregates of Euro-Mediterranean Regions-UPAT Methodology." Internal Report, Syner-G project 2009–2012.

Van Westen, C. J., L. Montoya, and L. Boerboom. 2002. "Multi-hazard Risk Assessment Using GIS in Urban Areas: A Case Study for the City of Turrialba, Costa Rica." *Proceeding of Regional Workshop on Best Practice in Disa*, Bali: Mitigation, 120–136.

Wells D. L., and K. J. Coppersmith. 1994. "New Empirical Relationships among Magnitude, Rupture Length, Rupture Width, Rupture Area, and Surface Displacement." *Bulletin of the Seismological Society of America* 84: 974–1002.

Zhang, L. M., F. Nadim, and S. Lacasse. 2013. "Multi-risk assessment for landslide hazards." In *Proceeding of Pacific*

Rim Workshop on Innovations in Civil Infrastructure Engineering, edited by S.-S. Chen and A. H.-S. Ang, 321–329. Taipei: National Taiwan University of Science & Technology. National Taiwan University of Science and Technology. ISBN: 978-986-03-7004-1.

Zhang, S. 2014. "Assessment of Human Risks Posed by Cascading Landslides in the Wenchuan Earthquake Area." PhD thesis, the Hong Kong University of Science and Technology, Hong Kong.

Zuccaro G., F. Cacace, R. J. S. Spence, and P. J. Baxter. 2008. "Impact of Explosive Eruption Scenarios at Vesuvius." *Journal of Volcanology and Geothermal Research* 178 (3): 416–453. doi:10.1016/j.jvolgeores.2008.01.005.